Evaluation of Thermal Properties of Ferromagnetic Core for Treatment of Solid Tumors by Electromagnetic Induction Hyperthermia

Elham Mohagheghpour (PhD)[1]*, Shahab Sheibani (PhD)[1], Reza Saber (PhD)[2], Mohammad Soliemanpoor (MSc Student)[3], Saeed Sarkar (PhD)[2], Amirhossein Nezamdust (BSc)[4]

[1]Radiation Applications Research School, Nuclear Science and Technology Research Institute, Tehran, Iran
[2]Research Center for Science and Technology in Medicine, Tehran University of Medical Sciences, Tehran, Iran
[3]Department of Energy Engineering, Sharif University of Technology, Tehran, Iran
[4]Department of Biomedical Engineering, Amirkabir University of Technology, Tehran, Iran

ABSTRACT

Background: Electromagnetic induction hyperthermia is a promising method to treat the deep-seated tumors such as brain and prostatic tumors. This technique is performed using the induction of electromagnetic waves in the ferromagnetic cores implanted at the solid tumor.

Objective: This study aims at determining the conditions of the optimal thermal distribution in the different frequencies before performing the in vitro cellular study.

Material and Methods: In this experimental study, the i-Cu alloy (70.4-29.6; wt%) was prepared and characterized and then the parameters, affecting the amount of induction heating in the ferromagnetic core, were investigated. Self-regulating cores in 1, 3, 6, and 9 arrangements in the water phantom with a volume of 2 cm^3 were used as a replacement for solid tumor.

Results: Inductively Coupled Plasma (ICP) analysis and Energy Dispersive X-ray Spectroscopy (EDS) show the uniformity of the alloy after 4 times remeling by vacuum arc remelting furnace. The Vibrating Sample Magnetometer (VSM) shows that the Curie temperature (T_C) of the ferromagnetic core is less than 50 °C. Temperature profile with a frequency of 100-400 kHz for 30 min, was extracted by infrared imaging camera, indicating the increase temperature in the range of 42 °C to 46 °C.

Conclusion: The optimum conditions with used hyperthermia system are supplied in the frequency of 100 kHz, 200 kHz and 400 kHz with 6, 3 and 1 seeds, respectively. It is also possible to induce a temperature up to 50 °C by increasing the number of seeds at a constant frequency and power, or by increasing the applied frequency at a constant number of seeds.

Keywords

Introduction

The process of hyperthermia is one of the methods of cancer treatment [1] since about 3000 BC [1, 2]. The term hyperthermia is a combination of two Greek words: hyper means increase and therm means heat [2, 3], referred to in various studies under different titles such as thermal therapy and thermotherapy [1]. Hyperthermia means a controlled increase in tumor temperature of 3-8 °C, usually used as adjunctive therapy to radiation therapy or chemotherapy, and

can increase tumor response to treatment without increasing side effects and significantly increase the survival rate of patients [1, 3-5]. At a temperature of about 40-45 °C, Thermal Enhancement Ratio (TER) is about 1.5-2, i.e. it is necessary to apply a radiation dose of 1.5-2 times to cause a certain number of damages to cells in the absence of hyperthermia that this also increases the dose received by the surrounding healthy tissues [6, 7]. Maximum TER is obtained when hyperthermia and radiation therapy are performed simultaneously [8, 9]. This is only possible if hyperthermia is used in combination with brachytherapy. This method is known as thermo brachytherapy, considered by many researchers due to the increased rate of elimination of defective cells due to increased sensitivity of cells to radiation therapy with increasing tissue temperature [5, 10-13].

One of hyperthermia process in thermo brachytherapy is performed using the induction of low-frequency electromagnetic waves in the ferromagnetic cores implanted at the solid tumor, with Curie temperature less than 50 °C, and on the surface of the core, adsorbed radioisotope performs that process of brachytherapy simultaneously.

Among the mentioned alloys, nickel-copper alloy has a history of more application than other alloys in thermo brachytherapy systems [4, 14]. Ni-Cu alloy was first developed in 1985 by Lilly et al. [15]. In 1989, Miller and colleagues investigated the effect of concomitant use of hyperthermia with the ferromagnetic core and I-125 Brachytherapy in the treatment of rabbit melanoma [16]. In 1992, Steeves and colleagues studied a combination of brachytherapy and hyperthermia to treat rabbit choroidal melanoma [17]. The results indicate a reduction in the dose required for treatment and the duration of treatment in the use of hyperthermia and brachytherapy simultaneously. Also, Brezovich et al. used Ni-Cu self-controlled ferromagnetic thermo-seed clinically, which did not show severe toxic-

ity or discomfort in patients, and the desired temperature in the tissue was created under the influence of different frequencies and magnetic fields [18]. In 2011, Adam Chicheł et al. conducted studies on the effects of heat therapy combined with brachytherapy for the treatment of breast cancer [19]. In 2012, Bhoj Gautam, Ishmael Parsai et al. compared the simulation by MCNP5 code with the reports of TG-43 working group and reported the results [20]. Finally, in 2016, Warrell, Parsai et al. studied the concurrent use of brachytherapy and hyperthermia in the treatment of prostate cancer [4], the results of which indicate an improvement in the treatment process in the simultaneous use of radiotherapy and thermotherapy.

Although there are several investigations on the use of hyperthermia by the induction of electromagnetic waves in Ni-Cu thermo seed alone or in combination with brachytherapy [1, 4, 14, 17, 18], none of the studies has investigated the effect of the number of cores used to generate the heat required for the hyperthermia process. Besides, the effect of the blood perfusion has been omitted, and the size of the water phantom was not considered equivalent to the dimensions of a solid tumor. While the presences of the blood flow in tumor tissue is one of the effective factors on the amount of induced temperature at the location of the thermo seed. Also, the size of the tumor affects the amount of induced heat and the way temperature is distributed in the tumor tissue.

In the present research, after preparation and characterization of Ni-Cu ferromagnetic core, the parameters affecting the thermal distribution within the target area was investigated. We report the effect of the number of cores in the different frequencies on the thermal distribution as well as the effect of the tissue blood perfusion on the thermal distribution in the phantom.

Material and Methods

In this experimental study, nickel-copper

alloy specimens were prepared by a vacuum arc remelting (VAR) furnace (Edmund Buhler). Nickel and copper rod with a purity of 99% and 99.9% respectively, were used to produce an alloy with a weight composition of 70.4% nickel and 29.6% copper. After surface deoxygenation and weighing, the metals were cleaned ultrasonically with acetone, ethanol, and deionized water prior to melting in furnace.

After creating a vacuum to a pressure of 10^{-5} Torr, melting was performed at a temperature of more than 2500 °C under argon gas. To increase uniformity in the alloy, each sample was re-melted 4 times. To form the alloy and produce the wire, a tensile device was used, and after several tensile steps using tensile doses, a wire with a diameter of 0.5 mm was created. Wire cutting was performed to develop 3.2 mm long pieces as ferromagnetic cores using a cutter.

Seeds in arrangements 1, 3, 6 and 9 were placed symmetrically in the center of the water phantom in the form of a rectangular cube with a square cross-section of 1 cm × 1 cm and a height of 2 cm (with a volume of 2 cm³ as a replacement for tumor tissue) and were fixed in the center of the coil of the hyperthermia system with the diameter equal 5 cm (Figure 1).

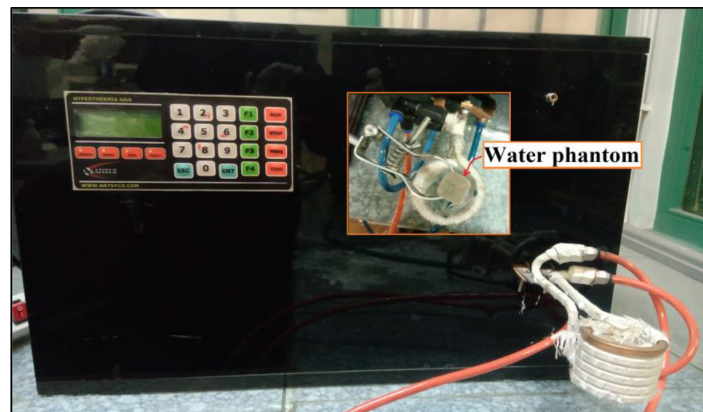Hyperthermia system for animal studies with the ability to generate a frequency in the range of 100-400 kHz, electromagnetic intensity between 2.4-12.9 kA/m and power from 100 to 1000 W (hyperthermia Equipment; Nano Technology System Corporation (NATSYCO)) was used to supply the electromagnetic field, as seen in Figure 1.

To observe the amount of induced heat in the ferromagnetic cores in the different conditions, Fluke TiS20 Infrared Camera was used and temperature measurement was conducted in the 3-5 min distance to apply the effect of blood flow in reducing the heat absorbed in tumor tissue by taking out the phantom from the coil.

Induction coupled plasma analysis (ICP; Optima7300-DV) and electron microscope (EDS; VEGA \\ TESCAN-LMU, RONTEC) were used to evaluate the uniformity of the alloy. The magnetic properties of the alloy were investigated using a vibrating sample magnetometer (VSM; Lak Shore 7400). The crystal structure of the alloy was investigated using X-ray diffraction (XRD; Siemens500 CuKα (λ=0.154 nm)).

Results

The X-ray diffraction result of Ni-Cu alloy produced using VAR furnace is shown in Figure 2. The spacing between (111) and (002) crystal plates in the alloy crystal lattice according to the Cohen, s method [21] is 2.06 Å and 1.78 Å, respectively.


Figure 1: View of hyperthermia system for animal studies and the cross-section sight of the water phantom that placed in the coil.

Figure 3 shows the results of EDS elemental analysis for one point of the surface and the concentration of nickel and copper elements in different parts of the alloy after 4 times remelting.
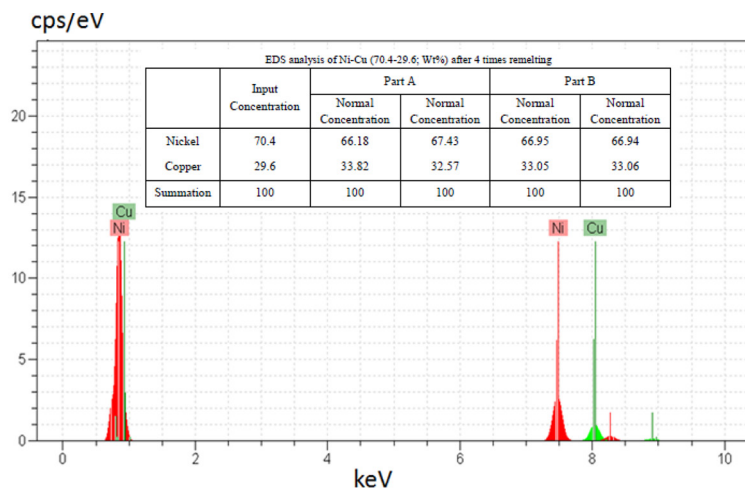
The study of the concentration of nickel and copper in a piece of dissolved alloy sample using ICP analysis showed the presence of 71% and 29% by weight of nickel and copper in the sample, respectively.

Differential scanning calorimetry (DSC) is commonly used to detect the Curie tempera-

ture [21]. Since in the present study, the transition enthalpy from ferromagnetic to paramagnetic is small and a pronounced peak is not observed, the DSC method was not used to determine the Curie temperature, and the magnetic properties of the alloy were investigated using VSM analysis. Although the determination of the Curie temperature is usually done using the information extracted from the VSM analysis and the line projection method, Arrott method, and modified Arrott method [22]. The study of the magnetic moment versus
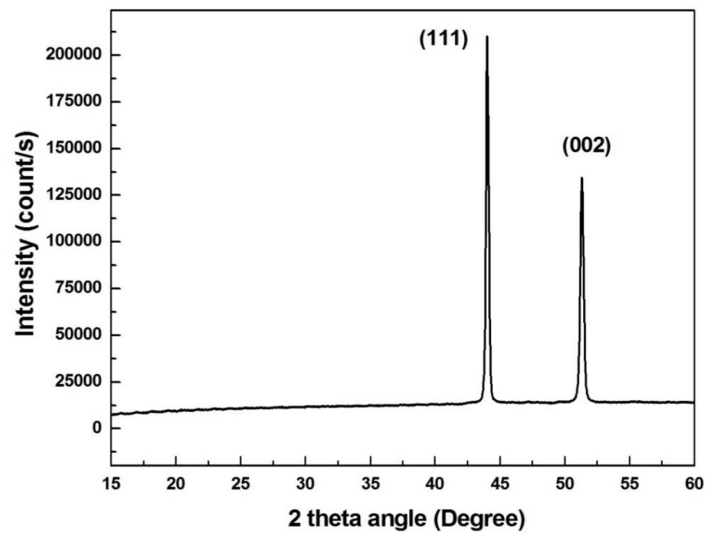
Figure 2: X-ray diffraction result for the nickel-copper alloy with weight composition (70.4-29.6%).

EDS analysis of Ni-Cu (70.4-29.6; Wt%) after 4 times remelting

	Input Concentration	Part A		Part B	
		Normal Concentration	Normal Concentration	Normal Concentration	Normal Concentration
Nickel	70.4	66.18	67.43	66.95	66.94
Copper	29.6	33.82	32.57	33.05	33.06
Summation	100	100	100	100	100

Figure 3: Results of Energy Dispersive X-ray Spectroscopy (EDS) analysis for Ni-Cu alloy after 4 remelting.

temperature curve in other studies has been performed under the 100 Oe magnetic field [22-24]. Also, according to the reported results by Hadimani et al. [23], the accurate measurement of the Curie temperature with the line projection method under a 1 Tesla magnetic field is difficult, and by drawing a tangent line in the curve, the Curie temperature is obtained higher than the real value. Since, in the present study, the used magnetic field was 1000 Oe, a diagram of magnetization changes with temperature change (dM/dT) was drawn and T_C was considered at the point where the dM/dT become zero to eliminate the effect of the applied magnetic field intensity [25, 26] (Figure 4).

As seen in Figure 4, the core temperature of Ni-Cu alloy is less than 50 °C, i.e. a temperature that the magnetic permeability of the studied Ni-Cu alloy decreases sharply [27]. In addition to the alloy composition, the intensity of the induction field, applied by controlling the power and frequency in the hyperthermia system, affects the Curie temperature that should be considered in the treatment design process. The extracted temperature profiles
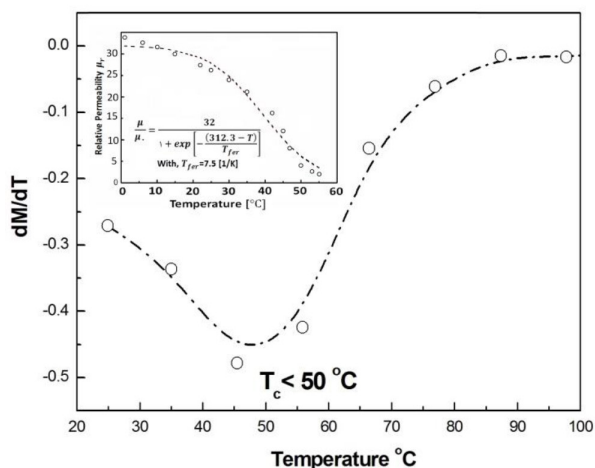
Figure 4: The ratio of magnetization changes to temperature changes dM/dT curve of Ni-Cu alloy measured at magnetic field of 1000 Oe; (inset: Variation of the relative permeability of the Ni-Cu alloy (70.4-29.6 ; wt%) with temperature [27]).

from the electromagnetic field induction at different frequencies (Figure 5) confirm this. As shown in Figure 5, at all frequencies studied, the seeds temperature increases over time and the induced temperature changes will be tiny after about 10 min. In addition, with increasing the number of seeds in the water phantom, the amount of induced heat increases. The Specific Loss Power (SLP) values reported in Table 1 confirm this.

In general, the thermal distribution resulted from the induction heating process of a ferromagnetic alloy is influenced by two heat transfer phenomena, including: 1) the heat produced due to the induction of eddy current and hysteresis loop in the ferromagnetic core under the influence of the alternating electromagnetic field, and 2) the heat transfer from the ferromagnetic core to the surrounding materials [27].

The amount of hysteresis loss is directly related to the volume of the core and the hysteresis loop area. Since the volume of the used ferromagnetic core in the present study is very small, the amount of hysteresis loss is negligible. The amount of heat produced in the thermo seed per unit volume (P_{FM}) due to the hysteresis loop is obtained according to Equation 1 [28]:

$$P_{FM} = \mu_0 f \int H dM \qquad (1)$$

In this equation, P_{FM} is the heat produced per unit volume by a ferromagnetic structure, f is frequency indicator, μ_0 is magnetic permeability and the integral indicates the area of the hysteresis loop. Since Ni-Cu alloy is a soft-magnetic alloy, in which the induced magnetic field (M) decreases rapidly when the external magnetic field (H) is cut off, and the integral value becomes very small. As a result, the amount of induced heat is drastically reduced due to the loss of hysteresis. Of course, as the applied frequency increases, the amount of heat produced increases slightly.

According to Faraday's law of electromagnetic induction, when an oscillating magnetic field intercepts a conductive object, an
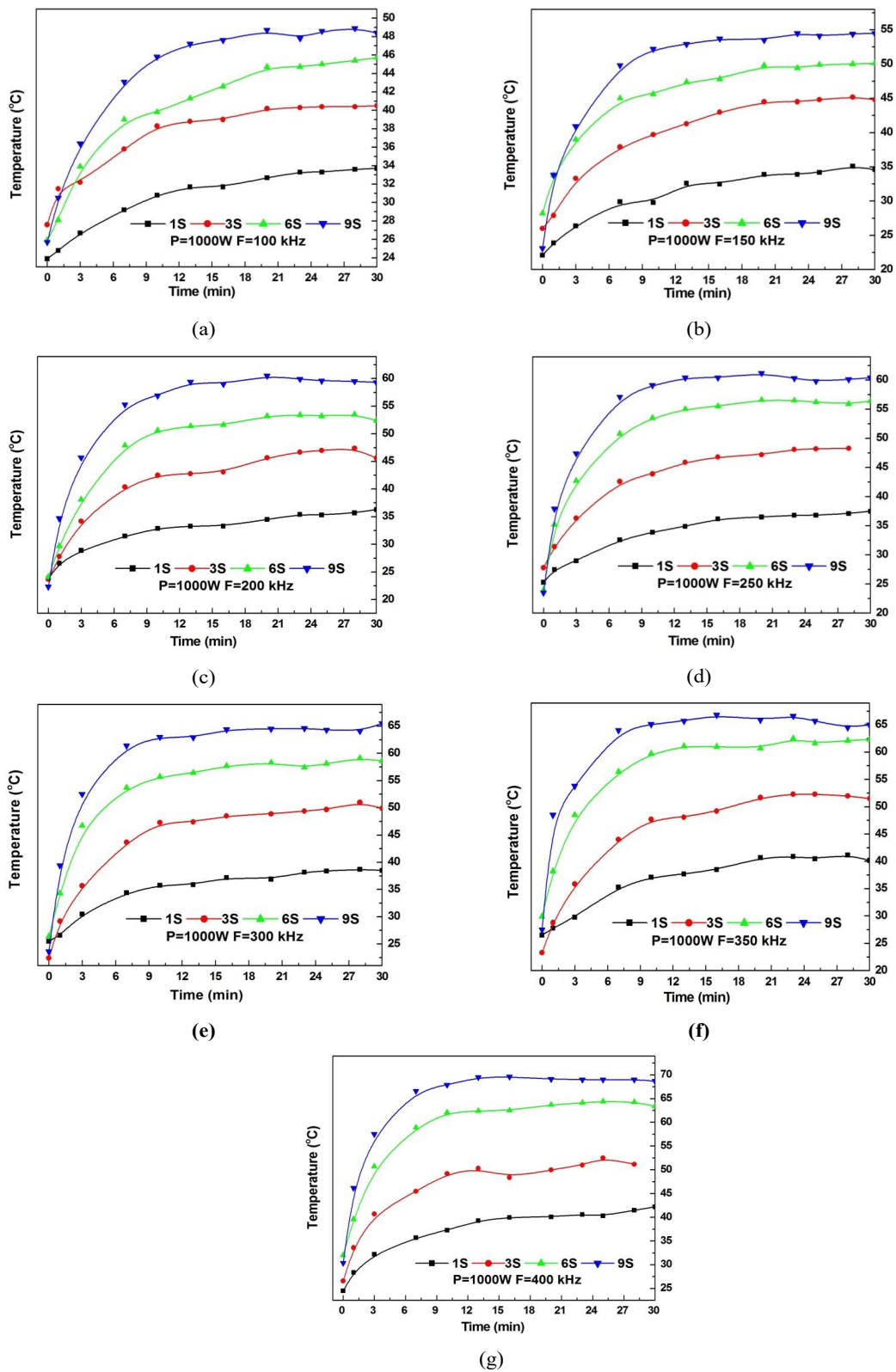
Figure 5: The extracted temperature-time profiles from the electromagnetic field induction at the central region of phantom (1×1 cm^2) with power=1000 W and in different frequencies; (**a**) 100 kHz, (**b**) 150 kHz, (**c**) 200 kHz, (**d**) 250 kHz, (**e**) 300 kHz, (**f**) 350 kHz and (**g**) 400 kHz.

Table 1: Applicable conditions of Ni-Cu ferromagnetic core (70.4-29.6%: W/W) for use in animal studies.

Power (W)	Frequency (kHz)	Magnetic field intensity (kA/m)	Number of seeds	Induction temperature	SLP (W/g)	Kind of hyperthermia	Suggestion terms
1000	100	11.6	3	40	0.078	Mild Hyper thermia	-
1000	100	11.6	6	46	0.068	moderate hyperthermia	✓
1000	100	11.6	9	48	0.12	Thermal abalation	✓
1000	150	11.8	3	45	0.067	moderate hyperthermia	✓
1000	150	11.8	6	50	0.107	Thermal abalation	-
1000	200	12.1	3	46	0.080	moderate hyperthermia	✓
1000	250	10.4	3	48	0.153	Thermal abalation	✓
1000	300	11.9	3	50	0.181	Thermal abalation	-
1000	350	12.9	1	40	0.054	Mild Hyper thermia	-
1000	350	12.9	3	52	0.117	Thermal abalation	-
1000	400	9.2	1	42.5	0.07	moderate hyperthermia	✓
1000	400	9.2	3	50	0.164	Thermal abalation	-

SLP: Specific Loss Power

electric current is induced, known as eddy current. The eddy current flows in the opposite direction of the inducing current. Resistive heating (Joule's heating) of the eddy current in the surface of the conductor generates heat. The heat power from induction heating in a conductor is obtained by Equation 2 [27]:

$$P_w = \sqrt{2}\,\pi\alpha L\rho R H_0^2 \frac{ber'\left(\sqrt{2}\,\alpha R\right)+bei\left(\sqrt{2}\,\alpha R\right)bei'\left(\sqrt{2}\,\alpha R\right)}{ber^2\left(\sqrt{2}\,\alpha R\right)+bei^2\left(\sqrt{2}\,\alpha R\right)} \quad (2)$$

Where 'L' is cylindrically-shaped implant of length and 'R' is cross-sectional radius, 'ρ' electrical resistance, H_0 is magnetic field strength and f is frequency.

In addition, $\alpha = \sqrt{\dfrac{\omega\mu}{\rho}}$, where ω is the applied frequency and μ is the magnetic permeability of the ferromagnetic core. The values of ber (x) and bei (x) are calculated using Equations 3 and 4:

$$ber(x) = 1 - \left(\frac{x}{2}\right)^4 \frac{1}{(2!)^2} + \left(\frac{x}{2}\right)^8 \frac{1}{(4!)^2} - etc \quad (3)$$

$$bei(x) = \left(\frac{x}{2}\right)^2 - \left(\frac{x}{2}\right)^6 \frac{1}{(3!)^2} + \left(\frac{x}{2}\right)^{10} \frac{1}{(5!)^2} - etc \quad (4)$$

And ber' and bei' are derivatives of ber and bei. Of course, the electrical resistance of the alloy also increases with increasing temperature, so that the slope of increasing the electrical resistance before T_C is higher than the slope after T_C [29]. Since the parameters μ and ρ vary with temperature change, Equation 2 is used in the simulation. In order to calculate the heat output from the ferromagnetic core per unit mass, assuming that the heat output from the induction heating of the core and the heat loss per unit mass are equal, a parameter called specific loss power (SLP) is used [26, 30] (Equation 5);

$$SLP = \left(\frac{CV_s}{m}\right) \times \left(\frac{dT}{dt}\right) \quad (5)$$

where C is the volumetric specific heat capacity of water, i.e. 4.18 J/(g °C), V_s is the sample volume, m is the magnetic material mass, and $\frac{dT}{dt}$ is the slope of temperature curve versus time at initial time interval [31]. The specific amount of power lost under different conditions is reported in Table 1.

As shown in Figure 4, the relative magnetic

permeability has sharply dropped in the temperature range of 50 °C, and increasing temperature is stopped. In addition, since the viability of cancer cells is reduced in T_C and their sensitivity to radiation therapy increases, the treatment will be more successful than when is used from radiation therapy alone. Of course, the induced temperature can increase by incremental frequency or strength of the applied magnetic field [31].

Based on the reported classification by Gaitham (Table 2), the hyperthermia performance at different temperatures is dependent to the physical and biological effects and cell killing mechanisms of each treatment [27]. Considering that the aim of the present study is to use hyperthermia as an adjunctive method and improve the response of tumor tissue to brachytherapy, the temperature supply conditions in the range of 41-46 °C are considered as favorable conditions for hyperthermia; and thermal ablation as an independent treatment method was performed at temperature above 46 °C (Table 1). The measured temperature was performed by an infrared camera after placing the seeds for 30 min in the electromagnetic field for hyperthermia process (Figure 6).

Discussion

The nickel-copper ferromagnetic core was produced with an acceptable weight percentage compared to the other reported researches [4, 14, 15, 18]; however, the weight composition of the alloy is not completely consistent with the input values. Since EDS is a qualitative analysis, and the reported concentrations have tiny deviation, the results are acceptable. Also, it can be concluded that the desired uniformity in the alloy is achieved by performing 4 times remelting.

According to the result of VSM analysis, the Curie temperature of the produced Ni-Cu ferromagnetic core similar to the other reports [4, 18] is less than 50 °C along with decreasing magnetic permeability. The mechanism of the thermal self-regulation in a conductor is due to a change in the magnetic permeability of the conductor with a change in temperature (Figure 4). In this way, as soon as the magnetic field is turned on, the alternating magnetic field induces an eddy current in the ferromagnetic material. The flow of the current on the surface of the core is limited by the skin effect caused by the alternating nature of the current. The resistive heating of the induced current produces heat. The temperature of the ferromagnetic material increases and the magnetic permeability decreases. Increasing the induction temperature leads to a decrease in the magnetic permeability of the ferromagnetic core. When the temperature of ferromagnetic material reaches the Curie temperature (T_C), it loses its ferromagnetism and becomes paramagnetic material. In other words, the magnetic susceptibility drops to zero at $T \geq T_C$.

Table 2: A summary of the treatment process by hyperthermia at different temperatures and their effect on living tissues [27].

Cell Killing Mechanism		Sensitization Effect of Heat			Direct Cell Killing
Therapy		39 °C < Mild Hyperthermia ≤ 41 °C	41 °C < Hyperthermia ≤ 46 °C		46 °C <Thermal Ablation
Treatment Duration	No time limit	> 4 hour	1-2 hours	15-60 min	< 10 min
Physical Effect	No Change	Change in optical properties of tissues			Necrosis, coagulation
Biological Effect	Growth	Increased perfusion, thermotolerence induction and improved oxigenation	Decreased perfusion and protein denaturation		Protein Denaturation
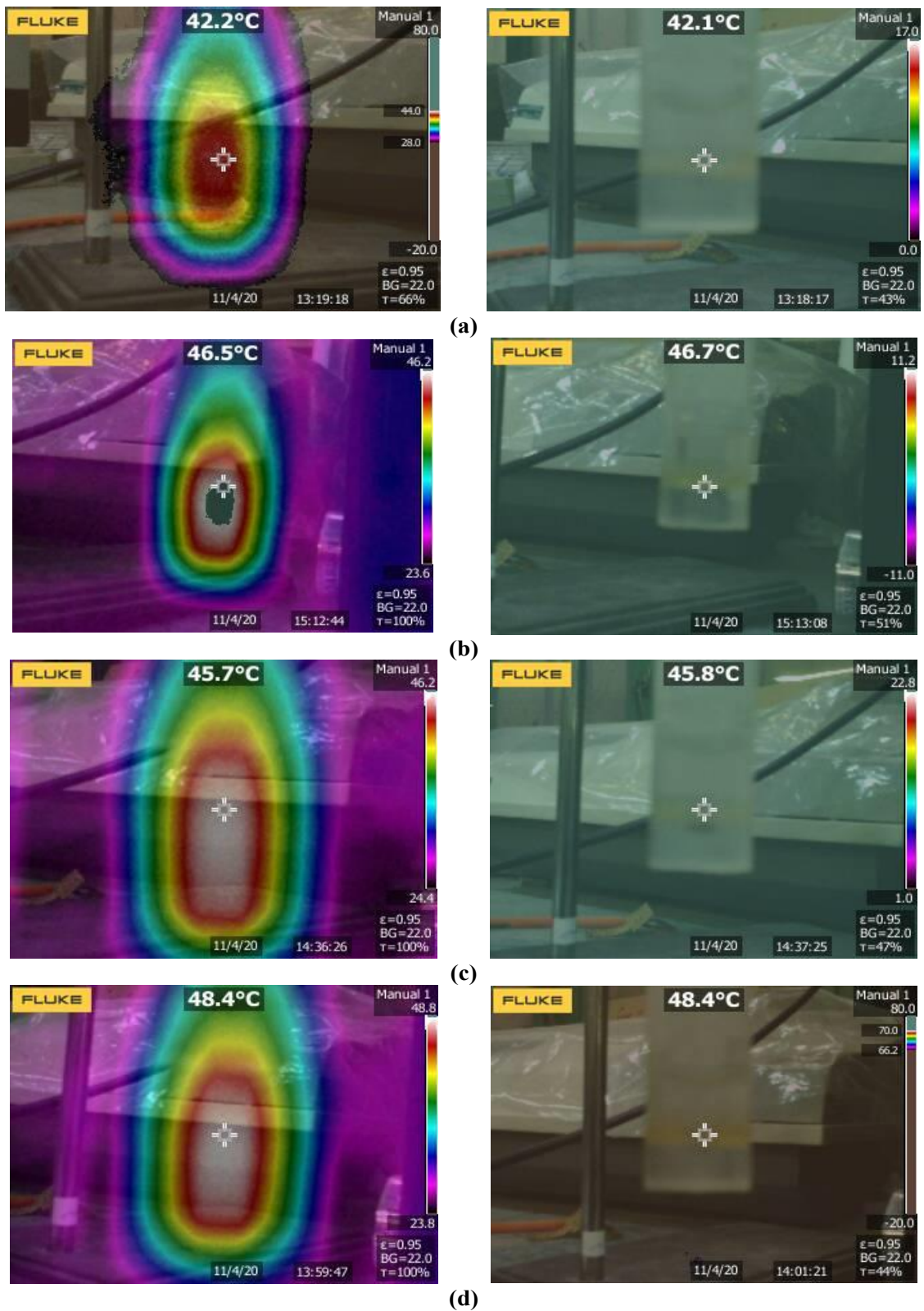
Figure 6: Suggestion terms for hyperthermia with Ni-Cu ferromagnetic core in power equal 1000 W and different frequency and number of seeds: (**a**) 1 seed (1S), F=400 kHz, (**b**) 3 seed (3S), F=200 kHz, (**c**) 6 seed (6S), F=100 kHz, (**d**) 9 seed, F=100 kHz.

In such condition, the ferromagnetic implant stops producing heating energy and the temperature starts decreasing. As the temperature decreases below T_C, the core material regains its ferromagnetic property and starts producing heat, and this cycle continues [27].

In addition to the alloy composition, the rate, at which heat is produced by a ferromagnetic core, depends on the intensity and frequency of the applied induction field. The rate of heat production generally goes up if any one of these parameters increases [18]. As shown in Figure 5, higher temperature induction is possible by incremental frequency at a constant number of ferromagnetic cores.

In this study, water was considered as tissue because the thermal conductivity and specific heat capacity of water are close to homogeneous, isotropic tissue without blood perfusion. Since the thermal distribution around the tissue is greatly affected by the amount of blood perfusion, in the present study, temperature measurement periodically was performed outside the coil for applying the effect of perfusion on the temperature reducing of the ferromagnetic core. Due to vascular disruption in solid tumors and impaired blood flow accumulated in tumor tissue as a result of dilation of blood vessels, more heat accumulation occurs in tumor tissue [1]. Hence, the temperature distribution of the tumor volume can be expected to be similar to water phantom. Also, although the blood flow and heterogeneous tumor tissue may affect the temperature distribution, the temperature self-regulating property of the core can compensate this defect; in this way, by the continues application of the magnetic field, creating eddy current leads to a re-increase of the implant temperature to the Curie temperature. Therefore, the temperature can be kept constant close to T_C. The tiny changes in the trend of temperature increasing in the ferromagnetic core after about 10 min (Figure 5) that also reported in the other researches [20, 27] reconfirm it.

The suggestion conditions in the present study, i.e. the use of hyperthermia as an adjunctive method for improving the response of tumor tissue to brachytherapy, are comparable to the those of reported in the other researches [4, 14, 18, 20, 27]. However, the intensity of the magnetic field is more than 20 kA/m in others literature, it was about 9.2-12.9 kA/m in the present study. Of course, in the present study, the size of the coil diameter is smaller than the other reports.

Conclusion

The nickel-copper ferromagnetic core with a weight percentage (70.4-29.6; wt%) and a Curie temperature of less than 50 °C was successfully fabricated using a VAR furnace.

Hyperthermia system used in the present study can induce temperature in the range of 42 °C to 50 °C in nickel-copper ferromagnetic core with a power of 1000 W, frequency of 100-400 kHz and the electromagnetic field range of 9.2-12.9 kA/m. The optimum conditions for hyperthermia as adjunctive therapy with this setup in the power of 1000 W are supplied in the frequency of 100 kHz, 200 kHz and 400 kHz with 6 seeds, 3 seeds and 1 seeds, respectively. It is also possible to induce a temperature up to 50 °C by increasing the number of seeds at a constant frequency and power; or by increasing the applied frequency at a constant number of seeds. In this case, hyperthermia can be used as an independent treatment.

Intra-tumor implantation of the self-regulating ferromagnetic core has the desirable characteristics, as follows: 1) creating and maintaining the desired temperature in a short time after the induction of magnetic field, 2) focusing temperature in the site of cores without worrying about damaging the adjacent healthy cells to tumor tissue, 3) reducing treatment time and dose due to the increased sensitivity of tumor tissue under hyperthermia compared to systems using radiation therapy alone,

Hence, using hyperthermia device with low-frequency electromagnetic waves is a suit-

able field for in vitro research to develop and expand an adjunctive treatment method of internal radiation therapy. Of course, since mass and size of the phantom affect the amount of induced heat and temperature profile of the ferromagnetic core in the electromagnetic field, employing a phantom with equivalent dimension to the tumor tissue is suggested for designing an in vitro treatment before in vivo studies.

Acknowledgment

We would like to thank Yasser Amoosi for offering help in reviewing and revising the manuscript for grammar and syntax.

Authors' Contribution

E. Mohagheghpour and Sh. Sheibani conceived the idea. All paper was written by E. Mohagheghpour. The method implementation was carried out by E. Mohagheghpour, M. Soliemanpoor and AH. Nezamdust. Results and Analysis was carried out by E. Mohagheghpour and R. Saber. The research work was proofread and supervised by E. Mohagheghpour, S. Sheibani and R. Saber. All the authors read, modified, and approved the final version of the manuscript.

Ethical Approval

Not applicable, because this article does not contain any studies with human or animal.

Conflict of Interest

None

References

1. Chichel A, Skowronek J, Kubaszewska M, Kanikowski M. Hyperthermia–description of a method and a review of clinical applications. *Reports of Practical Oncology & Radiotherapy.* 2007;**12**(5):267-75. doi: 10.1016/S1507-1367(10)60065-X.

2. Gas P. Essential Facts on the History of Hyperthermia and their Connections with Electromedicine [Internet]. arXiv [Preprint]. 2017 [cited 2017 October 2]. Available from: https://arxiv.org/abs/1710.00652.

3. Fratila RM, Fuente JM. Introduction to hyperthermia. Elsevier; 2019. doi: 10.1016/B978-0-12-813928-8.09997-X.

4. Warrell G, Shvydka D, Parsai EI. Use of novel thermobrachytherapy seeds for realistic prostate seed implant treatments. *Med Phys.* 2016;**43**(11):6033-48. doi: 10.1118/1.4964457. PubMed PMID: 27806619.

5. Jordan A, Scholz R, Wust P, Fähling H, Felix R. Magnetic fluid hyperthermia (MFH): Cancer treatment with AC magnetic field induced excitation of biocompatible superparamagnetic nanoparticles. *Journal of Magnetism and Magnetic Materials.* 1999;**201**(1-3):413-9. doi: 10.1016/S0304-8853(99)00088-8.

6. Emami B, Song CW. Physiological mechanisms in hyperthermia: a review. *Int J Radiat Oncol Biol Phys.* 1984;**10**(2):289-95. doi: 10.1016/0360-3016(84)90015-4. PubMed PMID: 6368492.

7. Oei AL, Vriend LE, Crezee J, Franken NA, Krawczyk PM. Effects of hyperthermia on DNA repair pathways: one treatment to inhibit them all. *Radiat Oncol.* 2015;**10**(1):1-3. doi: 10.1186/s13014-015-0462-0. PubMed PMID: 26245485. PubMed PMCID: PMC4554295.

8. Marino C, Cividalli A. Combined radiation and hyperthermia: effects of the number of heat fractions and their interval on normal and tumour tissues. *Int J Hyperthermia.* 1992;**8**(6):771-81. doi: 10.3109/02656739209005025. PubMed PMID: 1479203.

9. Stewart FA, Denekamp J. The therapeutic advantage of combined heat and X rays on a mouse fibrosarcoma. *Br J Radiol.* 1978;**51**(604):307-16. doi: 10.1259/0007-1285-51-604-307. PubMed PMID: 647188.

10. Rasaneh S, Dadras MR. The possibility of using magnetic nanoparticles to increase the therapeutic efficiency of Herceptin antibody. *Biomed Tech (Berl).* 2015;**60**(5):485-90. doi: 10.1515/bmt-2014-0192. PubMed PMID: 26146093.

11. Shvydka D, Gautam B, Parsai E, Feldmeier J. SU-FF-T-39: Investigating Thermal Properties of a Thermobrachytherapy Radioactive Seed for Concurrent Brachytherapy and Hyperthermia Treatments: Design Considerations. *Medical Physics.* 2009;**36**(6Part9):2528. doi: 10.1118/1.3181511.

12. Pankhurst QA, Connolly J, Jones SK, Dobson J. Applications of magnetic nanoparticles in biomedicine. *Journal of Physics D: Applied Physics.* 2003;**36**(13):R167.

13. Kuznetsov AA, Shlyakhtin OA, Brusentsov NA, Kuznetsov OA. "Smart" mediators for self-controlled inductive heating. *Eur Cells Mater.*

2002;**3**(2):75-7.

14. Parsai EI, Gautam B, Shvydka D. Evaluation of a novel thermobrachytherapy seed for concurrent administration of brachytherapy and magnetically mediated hyperthermia in treatment of solid tumors. *J Biomed Phys Eng.* 2011;**1**(1):5-16.

15. Lilly MB, Brezovich IA, Atkinson WJ. Hyperthermia induction with thermally self-regulated ferromagnetic implants. *Radiology.* 1985;**154**(1):243-4. doi: 10.1148/radiology.154.1.3964942.

16. Mieler WF, Jaffe GJ, Steeves RA. Ferromagnetic hyperthermia and iodine 125 brachytherapy in the treatment of choroidal melanoma in a rabbit model. *Arch Ophthalmol.* 1989;**107**(10):1524-8. doi: 10.1001/archopht.1989.01070020598048. PubMed PMID: 2803104.

17. Steeves RA, Murray TG, Moros EG, Boldt HC, Mieler WF, Paliwal BR. Concurrent ferromagnetic hyperthermia and 125I brachytherapy in a rabbit choroidal melanoma model. *Int J Hyperthermia.* 1992;**8**(4):443-9. doi: 10.3109/02656739209037982. PubMed PMID: 1402124.

18. Brezovich IA, Atkinson WJ, Lilly MB. Local hyperthermia with interstitial techniques. Cancer Res. 1984;44(10 Suppl):4752s-6s. PubMed PMID: 6380712.

19. Chicheł A, Skowronek J, Kanikowski M. Thermal boost combined with interstitial brachytherapy in breast conserving therapy–Assessment of early toxicity. *Rep Pract Oncol Radiother.* 2011;**16**(3):87-94. doi:10.1016/j.rpor.2011.02.004. PubMed PMID: 24376963. PubMed PMCID: PMC3863141.

20. Gautam B, Parsai EI, Shvydka D, Feldmeier J, Subramanian M. Dosimetric and thermal properties of a newly developed thermobrachytherapy seed with ferromagnetic core for treatment of solid tumors. *Med Phys.* 2012;**39**(4):1980-90. doi: 10.1118/1.3693048. PubMed PMID: 22482619.

21. Rabinkin A. Curie temperature of METGLAS magnetic alloys measured by different techniques. *IEEE Transactions on Magnetics.* 1987;**23**(6):3874-7. doi: 10.1109/TMAG.1987.1065772.

22. Robbins CG, Claus H, Beck PA. Transition from Ferromagnetism to Paramagnetism in Ni–Cu Alloys. *Journal of Applied Physics.* 1969;**40**(5):2269-73. doi: 10.1063/1.1657970.

23. Hadimani RL, Melikhov Y, Snyder JE, Jiles DC. Determination of Curie temperature by Arrott plot technique in Gd {sub 5}(Si {sub x} Ge {sub 1-x}){sub 4} for x> 0.575. *Journal of Magnetism and Magnetic Materials.* 2008;**320**:e696-8. doi: 10.1016/j.jmmm.2008.04.035.

24. Bettge M, Chatterjee J, Haik Y. Physically synthesized Ni-Cu nanoparticles for magnetic hyperthermia. *Biomagn Res Technol.* 2004;**2**(1):1-6. doi: 10.1186/1477-044X-2-4. PubMed PMID: 15132747. PubMed PMCID: PMC420488.

25. Ban I, Stergar J, Drofenik M, Ferk G, Makovec D. Synthesis of copper–nickel nanoparticles prepared by mechanical milling for use in magnetic hyperthermia. *Journal of Magnetism and Magnetic Materials.* 2011;**323**(17):2254-8. doi: 10.1016/j.jmmm.2011.04.004.

26. Chen Y, Wang Y, Liu X, Lu M, Cao J, Wang T. LSMO nanoparticles coated by hyaluronic acid for magnetic hyperthermia. *Nanoscale Res Lett.* 2016;**11**(1):1-6. doi: 10.1186/s11671-016-1756-3. PubMed PMID: 27914093. PubMed PMCID: PMC5135707.

27. Gautam BR. Study of dosimetric and thermal properties of a newly developed thermobrachytherapy seed for treatment of solid tumors [dissertation]. University of Toledo; 2013. Available from: http://rave.ohiolink.edu/etdc/view?acc_num=toledo1365181537.

28. Chaikin PM, Lubensky TC, Witten TA. Principles of condensed matter physics. Cambridge: Cambridge University Press; 1995.

29. Ho CY, Ackerman MW, Wu KY, Havill TN, Bogaard RH, Matula RA, Oh SG, James HM. Electrical resistivity of ten selected binary alloy systems. *Journal of Physical and Chemical Reference Data.* 1983;**12**(2):183-322. doi: 10.1063/1.555684.

30. Hatamie S, Parseh B, Ahadian MM, Naghdabadi F, Saber R, Soleimani M. Heat transfer of PEGylated cobalt ferrite nanofluids for magnetic fluid hyperthermia therapy: in vitro cellular study. *Journal of Magnetism and Magnetic Materials.* 2018;**462**:185-94. doi :10.1016/j.jmmm.2018.05.020.

31. Shaterabadi Z, Nabiyouni G, Soleymani M. Correlation between effects of the particle size and magnetic field strength on the magnetic hyperthermia efficiency of dextran-coated magnetite nanoparticles. *Mater Sci Eng C Mater Biol App.* 2020;**117**:111274. doi: 10.1016/j.msec.2020.111274. PubMed PMID: 32919638.